Accepted Manuscript

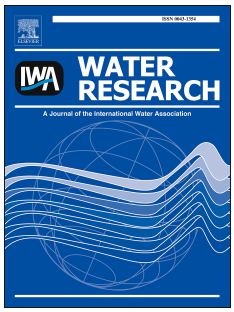

Inactivation of pathogenic microorganisms in freshwater using HSO_5^-/UV-A LED and HSO_5^-/M^{n+}/UV-A LED oxidation processes

Jorge Rodríguez-Chueca, Tatiana Silva, José R. Fernandes, Marco S. Lucas, Gianluca Li Puma, José A. Peres, Ana Sampaio

PII: S0043-1354(17)30497-9

DOI: 10.1016/j.watres.2017.06.021

Reference: WR 12976

To appear in: *Water Research*

Received Date: 20 March 2017

Revised Date: 6 June 2017

Accepted Date: 7 June 2017

Please cite this article as: Rodríguez-Chueca, J., Silva, T., Fernandes, José.R., Lucas, M.S., Puma, G.L., Peres, José.A., Sampaio, A., Inactivation of pathogenic microorganisms in freshwater using HSO_5^-/UV-A LED and HSO_5^-/M^{n+}/UV-A LED oxidation processes, *Water Research* (2017), doi: 10.1016/j.watres.2017.06.021.

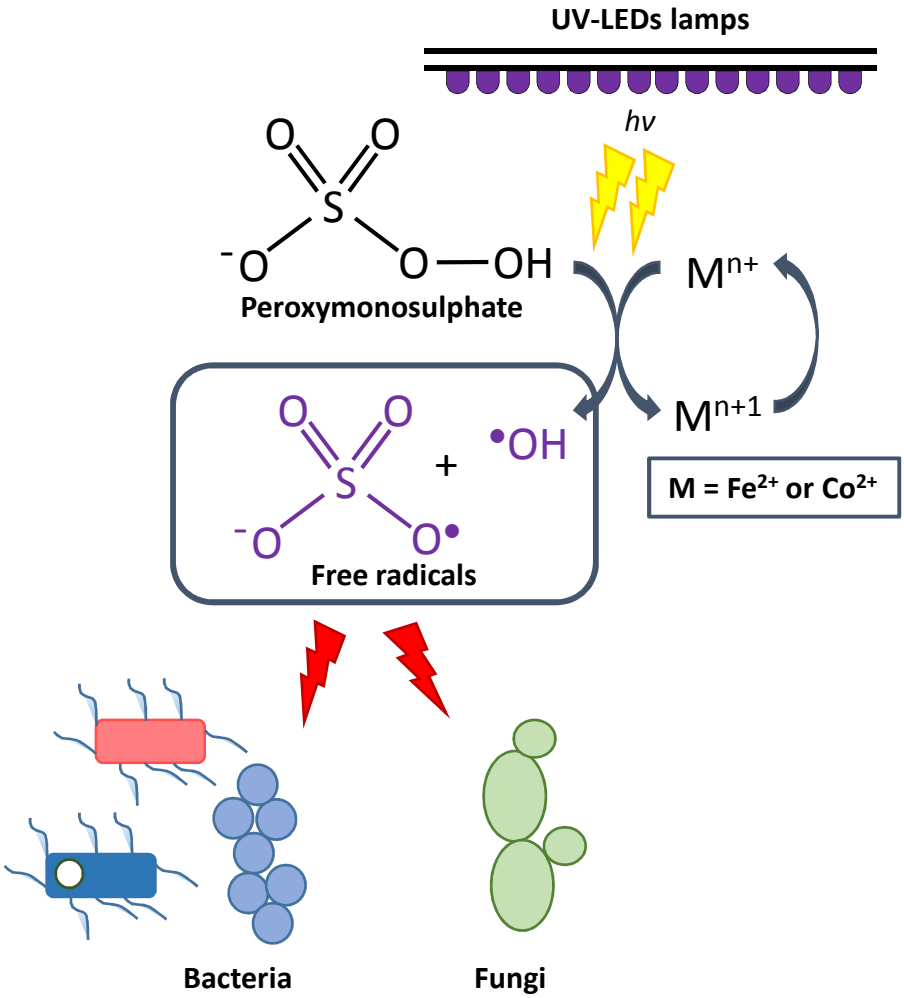
UV-LEDs lamps
hv
Peroxymonosulphate
M^{n+}
M^{n+1}
M = Fe^{2+} or Co^{2+}
•OH
Free radicals
Bacteria
Fungi

Inactivation of pathogenic microorganisms in freshwater using HSO_5^-/UV-A LED and HSO_5^-/M^{n+}/UV-A LED oxidation processes

Jorge Rodríguez-Chueca[1, 2], Tatiana Silva[3], José R. Fernandes[4, 5], Marco S. Lucas[1, 6]*, Gianluca Li Puma[6], José A. Peres[1], Ana Sampaio[3]

[1]Centro de Química de Vila Real, Departamento de Química, UTAD - Universidade de Trás-os-Montes e Alto Douro, Quinta de Prados, 5000-801 Vila Real, Portugal

[2]Department of Chemical and Environmental Technology, ESCET, Universidad Rey Juan Carlos, C/ Tulipán s/n, 28933 Móstoles, Madrid, Spain

[3]Centro de Investigação e de Tecnologias Agroambientais e Biológicas (CITAB), Departamento de Biologia e Ambiente, UTAD, Quinta de Prados, 5000-801, Vila Real, Portugal

[4]Departamento de Física, UTAD - Universidade de Trás-os-Montes e Alto Douro, Quinta de Prados, 5000-801 Vila Real, Portugal.

[5]INESC-TEC, Rua do Campo Alegre, 687, 4169-007, Porto, Portugal

[6]Environmental Nanocatalysis & Photoreaction Engineering, Department of Chemical Engineering, Loughborough University, Loughborough, LE11 3TU, United Kingdom

*CORRESPONDING AUTHOR

Dr. Marco S. Lucas

Email: m.p.lucas@lboro.ac.uk; mlucas@utad.pt

ABSTRACT

Freshwater disinfection using photolytic and catalytic activation of peroxymonosulphate (PMS) through PMS/UV-A LED and PMS/M^{n+}/UV-A LED [M^{n+} = Fe^{2+} or Co^{2+}] processes was evaluated through the inactivation of three different bacteria: *Escherichia coli* (Gram-negative), *Bacillus mycoides* (sporulated Gram-positive), *Staphylococcus aureus* (non-sporulated Gram-positive), and the fungus *Candida albicans*. Photolytic and catalytic activation of PMS were effective in the total inactivation of the bacteria using 0.1 mM of PMS and M^{n+} at neutral pH (6.5), with *E. coli* reaching the highest and the fastest inactivation yield, followed by *S. aureus* and *B. mycoides*. With *B. mycoides*, the oxidative stress generated through the complexity of PMS/M^{n+}/UV-A LED combined treatments triggered the formation of endospores. The treatment processes were also effective in the total inactivation of *C. albicans*, although, due to the ultrastructure, biochemistry and physiology of this yeast, higher dosages of reagents (5 mM of PMS and 2.5 mM of M^{n+}) were required.

The rate of microbial inactivation markedly increased through catalytic activation of PMS particularly during the first 60 seconds of treatment. Co^{2+} was more effective than Fe^{2+} to catalyse PMS decomposition to sulphate radicals for the inactivation of *S. aureus* and *C. albicans*.

The inactivation of the four microorganisms was well represented by the Hom model. The Biphasic and the Double Weibull models, which are based on the existence of two microbial sub-populations exhibiting different resistance to the treatments, also fitted the experimental results of photolytic activation of PMS.

Keywords: Peroxymonosulphate; microorganism inactivation; UV-A LED; kinetic modelling; PMS/M^{n+}/UV-A LED bacterial inactivation mechanism.

1. Introduction

Water disinfection is a complex process which is highly dependent on environmental factors and target microorganisms. *Escherichia coli* is a common indicator of fecal contamination in the analyses of water and wastewater (Parés and Juárez, 2002). This facultative anaerobic gram-negative bacteria is catalase positive and inhabits the intestinal tract of humans and other vertebrates and can be responsible for gastrointestinal diseases. In contrast, *Bacillus mycoides* is neither pathogenic nor a toxin producer. *B. mycoides* is a catalase positive, rod-shaped gram-positive bacteria, which has a typical rhizoid growth on solid media is catalase positive and able to ferment sugars such as glucose and maltose. It is a ubiquitous bacterium commonly found on plants, in soil, water, air, and decomposing plant tissue and frequently contaminates food, mainly vegetables. Under stress conditions *B. mycoides* forms endospores, which are resistant to physical and chemical factors such as high temperature, radiation and chemical disinfectants. *Staphylococcus aureus* is a gram-positive bacteria often found on skin, on skin glands, nasal and other mucous membranes, as well as on a wide range of food products such as milk and cheese that carry *S. aureus*. This catalase-positive and toxin producing bacteria is potentially pathogenic and can cause food poisoning when a food handler contaminates food or the food is not properly refrigerated. *Candida albicans* is a commensal fungus with a eukaryotic structure, commonly found in the oral and vaginal mucosa and in the gastrointestinal tract of humans. *C. albicans* lives in 80% of the human population, typically without causing harmful effects. However, excess of this fungus results in candidiasis (Calderone, 2002), causing opportunistic infections in immunocompromised patients, although it is rarely responsible for morbidity or mortality (Douglas, 1988).

Chlorination is the most commonly used disinfection agent worldwide (Le Chevallier and Au, 2004) and since its introduction over a century ago, human life expectancy has increased due to the prevention of waterborne diseases previously responsible for high mortality rates. The widespread use of chlorination has occurred as a result of its high rate of disinfection, its residual effect in the water, the low treatment cost, and the ease of handling. However, the generation of disinfection by-products (DBPs) (Rook, 1974) has raised significant concern among water treatment plants and regulators. More than 600 different DBPs have been reported in the literature (Richardson et al., 2007) the majority of which consists of trihalomethanes (THMs), chlorinated acetic acids, chlorinated ketones and halocetonitriles (WHO, 2008). DBPs are associated with public health risks via ingestion, inhalation, and skin absorption (Doederer et al., 2014). The majority of DBPs are a consequence of the chlorination of naturally occurring organic precursors such as humic substances (WHO, 2008; Grellier et al., 2015). Consequently, finding alternative effective mean of water disinfection which simultaneously avoid the generation of disinfection by-products has attracted the attention of many investigators (Venieri et al., 2015; Ferro et al., 2015; Giannakis et al., 2015).

Advanced Oxidation Processes (AOPs) are emerging as effective processes, which combine contaminants oxidation and disinfection. These are based on the generation of highly reactive species with a short lifetime such as hydroxyl radical-based AOPs (HR-AOPs), and sulphate radical-based AOPs (SR-AOPs). SR-AOPs based on sulphate radicals involves the application of chemical oxidants as persulphate salts, for example $Na_2S_2O_8$, $K_2S_2O_8$ and $KHSO_5$ (Wei et al., 2015). Peroxymonosulphate (HSO_5^-; PMS), is the active ingredient of potassium hydrogen monopersulphate ($2KHSO_5 \bullet KHSO_4 \bullet K_2SO_4$). The use of PMS as a disinfectant agent presents some advantages compared to hydrogen peroxide based HR-AOPs. Firstly, the oxidation

potential of ($E°_{HSO_5^-/HSO_4^-} = 1.82\,V$) is higher than that of hydrogen peroxide ($E°_{H_2O_2/H_2O} = 1.78V$), although lower than the potential of the hydroxyl radical ($E°_{\cdot OH} = 2.80\,V$). Furthermore, in contrast to H_2O_2 which requires special handling, potassium hydrogen monopersulphate is relatively stable at room temperature and easy to handle due to its solid state.

PMS alone is not an efficient disinfectant, but its action is significantly increased when it is catalytically (Eq. 1-3), thermally or photolytically (Eq. 4) activated, (Reactions 1-4) (Anipsitakis et al., 2008; Wang et al., 2011; Wang and Chu, 2012).

$$HSO_5^- + M^{n+} \rightarrow SO_4^{\bullet -} + M^{(n+1)+} + OH^- \quad (1)$$

M = Co^{2+}, Fe^{2+} and Ru^{3+}

$$HSO_5^- + M^{n+} \rightarrow [M^{(n+1)+}(SO_4^{\bullet})]^{n+} + OH^- \quad (2)$$

M = Ce^{3+}, Mn^{2+}, Ni^{2+}

$$HSO_5^- + M^{(n+1)+} \rightarrow SO_5^{\bullet -} + M^{n+} + H^+ \quad (3)$$

M = Ce^{4+}, Fe^{3+}, Mn^{3+}

$$HSO_5^- \xrightarrow{h\nu/\Delta} SO_4^{\bullet -} + HO^{\bullet} \quad (4)$$

Different authors have reported the catalytic activation of PMS through different transition metals such as Fe^{2+}, Co^{2+}, and Ni^{2+} (Anipsitakis et al., 2008; Wang and Chu, 2012; Anipsitakis and Dionysiou, 2003), but it is not clear which transition metal best activates PMS. For instance, the coupling of HSO_5^-/Fe^{2+} is one of the most commonly used combination, but presents disadvantages similar to those of the Fenton oxidation process, such as slow regeneration of Fe^{2+} and the production of ferric hydroxide sludge (Wang and Chu, 2012). The alternative coupling HSO_5^-/Co^{2+} presents some advantages in comparison to Fenton treatments, the most relevant of which being that it allows

using HSO_5^-/Co^{2+} without pH adjustment (Bandala et al., 2007; Yu et al., 2006), however the toxicity of Co^{2+} is a matter of concern in water treatment.

In this study, the effectiveness of SR-AOPs such as HSO_5^-/UV-A LED and HSO_5^-/M^{n+}/UV-A LED [$M^{n+} = Fe^{2+}$ or Co^{2+}] was assessed as alternative drinking water disinfection processes for the inactivation of a range of target microorganisms including the bacteria *E. coli* (gram-negative), *B. mycoides* (gram-positive endospore producer) and *S. aureus* (a non-endospore forming gram-positive) and the eukaryotic fungus *C. albicans*. The inactivation kinetics of these microorganisms was evaluated by nonlinear regression. This investigation into the disinfection of pathogen germs using PMS/UV-A LED and PMS/M^{n+}/UV-A LED systems contributes to future discussions regarding possible attack mechanisms of sulphate radicals in microbial inactivation.

2. Material and Methods

2.1. Microorganisms and chemicals

Wild strains of *E. coli* and *B. mycoides* were isolated from a water well and from soil, respectively, while collection strains of *C. albicans* and *S. aureus* were used (*C. albicans* ATCC 90028; *S. aureus* NCTC 10788/ATCC 6538). *E. coli* quantification was made over the selective culture media Chromocult agar (Merck) and *B. mycoides* and *S. aureus* determinations were carried out over a Luria-Bertani (LB) agar. LB agar was prepared by mixing tryptone (10 g/L; Difco®), NaCl (10 g/L; Merck), yeast extract (5 g/L; Gibco Europe) and agar-agar (1.5%; Merck). *C. albicans* was quantified using the yeast malt extract agar (YMA, Difco®): peptone (5 g/L), yeast extract (3 g/L), malt extract (3 g/L), glucose (10 g/L) and agar-agar (20 g/L).

Fresh liquid cultures were prepared in LB broth (bacteria) or Yeast-Malt broth (yeast) and incubated at 37 °C in a rotary shaker (150 r.p.m.) for 20 h. 1 mL of these microbial

143 suspensions were then added to water samples (500 mL) to obtain microorganisms
144 concentrations ranging from 10^5–10^6 colony-forming units (CFU)/100 mL.

145 All reagents used were analytical grade. Peroxymonosulphate and the metal catalysts
146 ($CoSO_4 \cdot 7H_2O$ or $FeSO_4 \cdot 7H_2O$) were purchased from Merck® and Panreac, respectively.
147 Sulphuric acid (H_2SO_4 Scharlau) and sodium hydroxide (NaOH Panreac) were used for
148 pH adjustment. UV-A LED radiation was used in combination with selected reagents to
149 increase the rate of formation of sulphate radicals.

150 **2.2. Disinfection experiments and UV-A LED photo reactor**

151 Freshwater samples (pH = 7.2 – 7.8; reduction potential (RP) = -0.82 mV; chemical
152 oxygen demand (COD) = 10 – 15 mg O_2/L; electrical conductivity (EC) = 230 – 250
153 µS; and total suspended solids (TSS) = 1 – 3 mg/L and turbidity = 0.4 – 1 NTU) were
154 collected from an artificial lake located at the UTAD campus (Vila Real, Portugal).
155 Sampling, handling and storage was carried out following the ISO 5667-3:2012
156 protocol.

157 Photo activation of PMS was carried out in lab-scale batch reactor illuminated with a
158 UV-A LED photo-system consisting of a matrix of 96 Indium Gallium Nitride (InGaN)
159 LEDs lamps (Roithner RLS-UV370E) which illuminated an area of (11 x 7) cm^2. Each
160 LEDs with light peak emission at 370 nm, consumed 80 mW at an applied current of 20
161 mA. The LED array optical emission was controlled by a pulse width modulation
162 (PWM) circuit, which determined the electric current supplied to each array LED. The
163 square waveform current supplied had two states: 0 mA (LED emission OFF state) and
164 30 mA (LED emission ON state) and frequency of 350 Hz. The PWM module allows
165 the configuration of the ON state time duration in each cycle between 0 and 100% of the
166 cycle period and, consequently, the emitted average optical power was controlled

between 0 and 100 mW. The photon irradiance was measured using a UV enhanced Si-photodetector (ThorLabs PDA155) in a configuration that replicated that used in the photoreactor. In this system, the output optical power was controlled using a pulse width modulation (PWM) circuit and the RMS current intensity was measured with a multimeter (UniVolt DT-64). The disinfection experiments were carried out with a RMS current intensity of 240 mA, corresponding to a UV irradiance of 23 W/m^2 and a photon flux of 5.53×10^{-7} Einstein/s.

The PMS/UV-A LED and PMS/M^{n+}/UV-A LED experiments were carried out using 0.1 mM as an optimal dosage of PMS and transition metals [Fe^{2+} and Co^{2+}] in bacteria inactivation (Rodríguez-Chueca et al., 2017). However, the optimal dosage for removing *C. albicans* was 5 mM for PMS and 2.5 mM for transition metals.

2.3. Analytical determination

Chemical oxygen demand (COD) was measured according to Method 410.4 of the US EPA (EPA, 1993), using a HACH DR/2400 portable spectrophotometer. The pH and the reduction potential were determined by a HANNA pH 209 laboratory meter following Standard Method 4500-H^+-B and 2580 (Eaton et al., 2005), respectively. Conductivity was measured using a Crison Basic as indicated in ISO 7888:1985. Turbidity was measured according to ISO 7027:1999 using a HACH 2100 IS Turbidimeter and the Total Suspended Solids (TSS) were measured by spectrophotometry according to Standard Method 2540D (Eaton et al., 2005) using a HACH DR/2400 portable spectrophotometer.

E. coli, *B. mycoides*, *S. aureus* and *C. albicans* concentrations were determined by the spread plate method (Standard Method 9215C; Eaton et al., 2005) after a serial 10-fold dilution in sterilized saline solution (NaCl 0.9%). Aliquots of diluted samples were

plated on Chromocult agar (Merck) for *E. coli* and LB agar for *B. mycoides* and *S. aureus*. YMA was used to quantify *C. albicans*. Colonies were counted after 24 h of incubation at 37 ºC. The microorganism detection limit (DL) was 1 CFU/mL. Microbial regrowth was estimated after the sample storage at room temperature for 24 and 48 h, after the sampling time, *t. B. mycoides* endospores were stained using the differential staining (Schaeffer and Fulton, 1933). Briefly, bacterial suspensions were fixed by heat and stained with malachite green (6 minutes), and after cooling the slide, washed with tap water and stained with safranin (30 seconds). This procedure stained in green and in red the endospores and vegetative or mother cells, respectively. Endospores were observed under a Nikon Eclipse E600 light microscope, at 1000 x magnification.

2.4. Kinetic modeling

Mathematical inactivation models applied to describe the microorganism inactivation kinetics (Table 1) were fitted using Microsoft® Excel: Solver and GInaFiT (Geeraerd and Van Impe Inactivation Fitting Tool) (Geeraerd et al., 2005),

Table 1

3. Results and discussion

3.1. Bacteria inactivation

PMS/UV-A LED treatments

Figure 1 shows the inactivation of bacteria with the PMS/UV-A LED process (*E. coli* Figure 1a; *B. mycoides* Figure 1b; *S. aureus* Figure 1c). The highest rate of microbial inactivation (4.81 to 7.28 log after 90 min, depending on the bacteria) was achieved using PMS in the range 0.1 to 0.5 mM and with UV-A LED irradiation. Higher PMS concentrations up to 10 mM yielded lower inactivation rates (data not shown). The application of PMS in dark (PMS/Dark) brought about a considerable reduction of the

E. coli population (5.59 log in 90 min) but the bacteria inactivation with UV-A LED radiation alone was negligible (< 0.50 log). *B. mycoides* cells (Figure 1b) were more resilient than *E. coli* (Figures 1a) at equal PMS concentration. Increasing the PMS concentration from 0.1 to 0.5 mM resulted in a faster inactivation of *B. mycoides*, however, the rapid rate observed during the first minute was followed by a significant reduction of the inactivation rate (2.19 log after 90 min) due to the formation of endospores which exhibit stronger resistance to oxidation. The endosporogenesis was observed and confirmed, after staining under microscope (Schaeffer and Fulton, 1933) for the samples collected during the first 10 minutes of contact time. In *B subtilis*, the formation of asymmetric division and forespore with its septa has been observed after 15 minutes (Ojkic et al., 2016) and the release of mature endospores may occur 90 minutes after the initial formation of endospores (Serrano et al., 2011).

Finally, the results for *S. aureus* (Figure 1c) demonstrated also the effectiveness of the PMS/UV-A LED process in comparison to PMS/Dark and UV-A LED alone. The inactivation rate with (0.1 mM PMS) was similar to that observed on *B. mycoides*, however, in contrast the rate observed at higher PMS concentration (0.5 mM) was higher than that observed with 0.1 mM.

Figure 1

The kinetic parameters (k and δ) obtained after the fitting of eight different mathematical bacteria inactivation models on the results obtained with the PMS/UV-A LED and PMS/Dark processes, are presented in Table 2. The Hom model (H) fitted the inactivation results for all bacteria. The Hom's kinetic rate constants for the PMS/UV-A LED inactivation of the bacteria were as follows: *E. coli* (0.39 min^{-1}) > *S. aureus* (0.33 min^{-1}) > *B. mycoides* (0.06 min^{-1}) and in the absence of radiation (PMS/Dark) were *S.*

aureus: *E. coli* (0.18 min^{-1}) > *B. mycoides* (0.15 min^{-1}) > *S. aureus* (0.003 min^{-1}). In addition, Biphasic and Biphasic with Shoulder models satisfactorily fitted the inactivation results obtained for *E. coli* and *S. aureus* populations. These models, as well as the Double Weibull model, are based on the hypothesis that bacterial population is divided into two subgroups, which differ in their resistance to the treatments.

Table 2

In general, the application of PMS as an alternative method for microorganism inactivation and water disinfection has been rarely reported in the literature. PMS treatment of groundwater contaminated with *E. coli* and *Enterococcus* sp. yielded more than 3 log inactivation after 15 minutes of exposure time, using 4 mg/L of PMS (6.50 µM) (Bailey et al., 2011). Although *Enterococcus* is also a Gram-positive like *B. mycoides*, higher concentrations of PMS are needed to inactivate more resilient Gram-positive such as the sporulated bacteria.

PMS/M^{n+}/UV-A LED treatments

Figure 2 shows the bacterial inactivation through the catalytic activation of 0.1 mM PMS without or with UV-A LED/M^{n+}. The activation of PMS UV-A LED by a transition metal [Fe^{2+} or Co^{2}] increased the inactivation rate of *E. coli* (Figure 2a): the combination of PMS with Fe^{2+} reached 2.60 log during the first minute of treatment, and the detection limit (6.68 log) after 45 minutes of treatment. The results obtained were similar to those observed with Co^{2+} as PMS activator. An identical pattern was observed for *B. mycoides* during the first few minutes of treatment with PMS/M^{n+}/UV-A LED (Figure 2b). Nevertheless, after 30 min (2.30 and 3.04 log with Co^{2+} and Fe^{2+}, respectively) the inactivation yield stabilized and in contrast to the treatment with PMS/UV-A LED, it reached the detection limit (DL) at a longer time after 120 min,

263 Therefore, the highest inactivation values obtained were 3.22 and 3.42 log with Co^{2+}
264 and Fe^{2+} respectively.

265 Finally, the inactivation behaviour of *S. aureus* followed a different behaviour (Figure
266 2c). The combination PMS with Co^{2+}/UV-A LED considerably increased the
267 inactivation rate of *S. aureus* (6.10 log), compared to the treatment with non-activated
268 PMS/UV-A LED radiation (4.80 log), or the PMS/UV-A LED combined with Fe^{2+}
269 (3.17 log).

270 **Figure 2**

271 In order to increase the microbial inactivation rate and reduce the inactivation time, a
272 second dose of reagents (PMS and the transition metal) was supplemented at the 15th
273 min of treatment (Figure 3). As observed in Figure 3a, this second dose did not result in
274 an increase of the inactivation of *E. coli*, and the detection limit was reached almost at
275 the same time as for the treatments carried out with only one addition of reagents. The
276 low resistance of *E. coli* to the oxidative treatments made the second dose of reagents
277 redundant. For *B. mycoides*, the second dose of reagents diminished the inactivation
278 rate. The increase of oxidative stress triggered the sporulation process, increasing the
279 physiological resistance of the *B. mycoides* population (Figure 3b) and the generation of
280 endospores was confirmed by staining. Finally, Figure 3c shows the inactivation of *S.*
281 *aureus*, which dramatically increased with the second dosing of reagents with the
282 combination of PMS with Fe^{2+}. However, such effect was not observed with the
283 combination PMS with Co^{2+} which showed a negligible rate increase. The DL was
284 achieved at 120 min in both cases, i.e. PMS with Fe^{2+} or Co^{2+}. Although authors as
285 Spuhler et al. (2010) reported the *E.coli* inactivation efficiency of Fe(II)/hυ and

Fe(III)/hυ systems, this effect has not been observed in this research (data not shown), nor Fe(II) neither Co(II).

Figure 3

Tables 3 and 4 show the kinetic parameters (k and δ) obtained after the fitting of the inactivation results with the PMS/M^{n+}/UV-A LED process with one and two additions of reagents with the different mathematical models. As shown, only the Hom model could fit all the inactivation results. Comparing the values of the Hom model kinetic constants (Table 2 and Table 3), the combination of Co^{2+} or Fe^{2+} with PMS and UV-A LED radiation resulted in a significant increase in the inactivation rate of all bacteria. As an exception the PMS/Fe^{2+}/UV-A LED (0.05 min^{-1}) was less effective than the PMS/UV-A LED (0.33 min^{-1}) process for the inactivation of *S. aureus*. This behavioural pattern had already been observed in Figure 2c. In general, the highest kinetic constants were achieved through the catalytic activation of PMS with Co^{2+}, the exception being the case of *B. mycoides*, where a higher inactivation rate was obtained using Fe^{2+}.

With double dosing of reagents, the DL was attained more quickly. However, the kinetic constants were slightly lower (Table 4) than those obtained with a single dose (Table 3), except for *S. aureus*. For *S. aureus*, a second dose of reagents increased the inactivation rate (k and δ) in almost all models, both with Co^{2+} or Fe^{2+}.

Table 3

Table 4

Anipsitakis et al. (2008) reported the use of PMS in combination with traces of Co^{2+} as an *in situ* swimming-pool sanitizer (Anipsitakis et al., 2008). The application of 25 mg/L of PMS and 0.1 mg/L of Co^{2+} was proven efficient, but with a rather slow

disinfection rate. Under the pool water conditions, a 4-log kill of *E. coli* was achieved after 60 min of treatment. This result does not meet the requirements as an EPA-registered swimming pool sanitizer, which requires 6-log kill of *E. coli* ATCC 11229, and of *Enterococcus faecium* ATCC 6569, within 30 seconds. Although still short of the standard required for use as a swimming-pool sanitizer, the results presented in this manuscript show that the application of 0.1/0.1 mM PMS/Co^{2+}/UV-A LED radiation reached almost 3 log inactivation of *E. coli* after just 1 min of treatment, therefore such process could potentially be used in a combined water disinfection process.

The mechanism of attack of the sulphate radical on bacteria is still unknown. However it has been hypothesized that the increase of oxidative conditions around the bacteria cells involves over-stress conditions that results in their inactivation. Understanding the process is made difficult by the necessity to take into account the large number of exogenous agents able to attack bacteria, such as sulphate and hydroxyl radicals, UV-A radiation, and the transition metals [Fe^{2+} and Co^{2+}]. Figure 4 is an adaptation from the research of Ma et al. (2009) and Spuhler et al. (2010), showing the possible pathways in the inactivation of *E. coli* (Gram-negative bacteria) using PMS/UV-A LED and PMS/M^{n+}/UV-A LED treatments. Taking into account each oxidative agent individually, there are a variety of possible oxidative effects on the cell. For instance, UV-A light can damage catalase (CAT) and superoxide dismutase (SOD) enzymes, which are responsible for the elimination of metabolic generated H_2O_2 and $O_2^{\bullet-}$, so their dysfunctioning could increase the intracellular concentration of these ROS species (Imlay, 2008). Furthermore, endogenous and exogenous photosensitizers (PS) can absorb UV-A radiation, reach an excited state and attack biomolecules or react with oxygen generating ROS species (Acra et al., 1990; Reed, 2004) causing oxidative damage to the bacteria. In addition, UV-A radiation can damage iron containing

proteins like Ferritin, leading to the intracellular release of Fe^{2+} which enhanced free iron pools that will scavenge the heme and iron released by subsequent oxidising (UV-A) treatments (Hoerter et al., 1996; Tyrrel et al., 2000).

While UV-A radiation causes oxidative stress to the cell, other agents, such as the transition metals, such as Fe, Co, Ni, Cu, etc. can also provoke significant damage. Although some transition metals are essential oligonutrients satisfying important biological functions of microorganisms, an excess of them can be lethal (Blaha et al., 2011). The membranes of bacteria are formed by different proteins whose functions are related to the selective transport of molecules into the cytosol. The location of the periplasmic space differentiates Gram-negative from Gram-positive bacteria, which in the former is located between the outer and the inner membranes. In consequence, in Gram-negative bacteria the, metals have to diffuse through the periplasm before entering the cytosol. The porins, trimeric proteins embedded in the outer membrane (OM), allow the passive diffusion of metal ions across the OM (Figure 4). In order to meet cellular metal demands, however, the cytosol must effectively concentrate metal ions. Consequently, there are high-affinity active transport systems in both membranes (outer and inner) and in the plasma, the purpose of which is to transport and release metal ions into the cytosol (Ma et al., 2009). Any excess concentration of Fe^{2+} or Co^{2+}, resulting from the PMS/M^{n+}/UV-A LED treatments, may increase the mortality of the bacteria. Usually bacteria deploy detoxification mechanisms to remove excess metals. In *E. coli*, RcnA is an efflux pump responsible for both Ni and Co detoxification, whilst the Cation Diffusion Facilitator (CDF) is responsible for Fe. RcnA confers resistance to Ni and Co, and its expression is induced by these two metals and not by other divalent cations (Rodrigue et al., 2005). So, it could be hypothesised that defective operation of these pumps as a consequence of Co^{2+} or Fe^{2+} excess may contribute to bacteria

inactivation. Another hypothesis related to Fe^{2+} is based on the diffusion of extracellular Fe^{2+} into the cytoplasm and the subsequent reaction with intracellular H_2O_2 via a Haber-Weiss reaction, generating hydroxyl radicals that directly attack cellular DNA.

Figure 4

Perhaps the most important contribution to the cellular attack is provided by sulphate and hydroxyl radicals generated in the PMS/UV-A LED and PMS/M^{n+}/UV-A LED processes. The literature regarding the use of sulphate radicals in microbial inactivation is still scarce and an understanding of their attack mechanism is based on the surmise that their behaviour may be similar to that exerted by hydroxyl radicals. Sulphate and hydroxyl radicals react with the cellular constituents responsible for lipid peroxidation in intracellular and cellular membranes, enhancing permeability and inactivation (Spuhler et al., 2010; Reed, 2004; Cabiscol et al., 2000). It is also well-known that hydroxyl radicals are the only ROS which can directly damage DNA (Sattlet et al., 2000), and there are no reports on the action of sulphate radicals on DNA.

Although the majority of the literature reports the oxidative stress on *E. coli* (Gram-negative bacteria), the relevant mechanisms could be quite similar for other bacteria, even for Gram-positive bacteria, and consequently oxidative stress could influence them in a similar way. There are important structural differences between both types of bacteria, and these are shown in Figure 5. As a result of these differences, Gram-positive bacteria are generally more resistant than Gram-negative bacteria (Madigan et al., 2012). However, both types of bacteria could also possess similar efflux pumps, the aim of which is to maintain homeostasis in the cytoplasm, and thus share the same vulnerability to pump disruption. Finally, the hypothesis that both sulphate and

hydroxyl radicals lethally attack the bacteria cell membranes and DNA and prevent their re-growth is proposed.

Figure 5

3.2. *Candida albicans* inactivation

Figure 6 shows the inactivation of the fungus *C. albicans* using the PMS/UV-A LED (Figure 6a) and PMS/M^{n+}/UV-A LED (Figure 6b) processes. Lower concentrations of PMS (0.1 and 0.5 mM) were ineffective on the inactivation of *C. albicans*, while a tenfold increase (5 mM) resulted in a significant reduction of *C. albicans* (Figure 6a). Under these operational conditions, combined with UV-A LED, the DL was reached at 120 minutes (5.61 log).

The inactivation rate of this species was drastically improved using a combination of PMS with a transition metal (Fe^{2+} or Co^{2+}), especially with Co^{2+}. As shown in Figure 6b, after 15 minutes of contact time 2 log inactivation was achieved with the combination of 5 mM of PMS with 2.5 mM of Fe^{2+}. When Co^{2+} was used as a metal catalyst for PMS, 4.30 log inactivation was observed during the first minute of contact time, and the DL was reached after 30 minutes (5.30 log). The fast inactivation observed with PMS and Co^{2+} did not warrant further doses of reagents. However, a second dose of PMS and Fe^{2+} supplemented after the 15^{th} minute (Figure 6b) produced a more rapid rate of inactivation to the DL (after 30 minutes, 5.64 log).

Figure 6

Table 5 shows the kinetic parameters (k and δ) obtained after fitting the mathematical models to the inactivation results of *C. albicans* obtained with the PMS/UV-A LED and PMS/M^{n+}/UV-A LED processes, with either one or two reagents doses. As previously observed in the kinetic parameters of bacteria, the Hom model fitted the inactivation

406 results of *C. albicans* (Table 5). The inactivation rate of *C. albicans* increased 10-fold
407 with the addition of Fe^{2+} (0.90 min^{-1}) and 40-fold with the addition of Co^{2+} (4.23 min^{-1})
408 in combination with PMS, in comparison to the results obtained with the PMS/UV-A
409 LED process (0.09 min^{-1}). A further dose of of PMS and Fe^{2+} increased the inactivation
410 rate of *C. albicans*, (1.46 min^{-1}).

411 **Table 5**

412 Kühn et al. (2003) reported that *C. albicans* was more resilient, when compared to other
413 microorganisms such as *E. coli*, *Pseudomonas aeruginosa*, *S. aureus* and *Enterococcus*
414 *faecium*, when treated with TiO_2/UV photocatalysis. Although *C. albicans* is a
415 commensal constituent of normal gut flora, this fungus can be pathogenic and can
416 developed defence mechanisms against the immune cells of the host, resisting the high
417 oxidative stress caused by these cells (Jiménez-López and Lorenz, 2013). Studies of the
418 interaction model of *C. albicans* versus macrophages, have shown that the fungus is
419 resistant to stress caused by ROS and nitrogen reactive species (RNS) generated by
420 macrophages. *C. albicans* encode a catalase (cat1), and six superoxide dismutases
421 (SOD), with three of them extracellular (Sod4-6) and are able to detoxify the ROS
422 released by macrophages (Frohner et al., 2009). Defences against intracellular RNS are
423 in the form of three flavohemoglobins enzymes (Ullmann et al., 2004). Therefore, it is
424 possible to hypothesize that the natural resistance of *C. albicans* to macrophages may
425 induce a higher resilience than bacteria to sulphate radicals (SOS). Metal toxicity in
426 *Saccharomyces cerevisiae* are involved in ROS generation, lipid peroxidation, and
427 depletion of glutathione (GSH), a major antioxidant in eukaryotic cells. Yeast seems to
428 use the same mechanisms to resist either iron or cobalt stress (Wang et al., 2017; Stadler
429 and Schweyen, 2002). In the first line of defence, yeasts increased cobalt sequestration
430 in the vacuole and later increased the expression of genes involved in the oxidative

stress (Stadler and Schweyen, 2002; Conklin et al., 1992; Pimentel et al., 2014). More recently, Wang et al. (2017), reported that *S. cerevisiae* yeast cells treated with Cd^{2+} also increased intracellular Ca^{2+} levels and provoked the collapse of the mitochondrial membrane potential. Cobalt also significantly inhibited *C. albicans* clamidospore germination when compared to other metals such as iron and zinc (Hazen and Cutler, 1983). These responses may explain the combined effect of PMS and metal (either Fe^{2+} or Co^{2+}), which was reflected by a 10-fold and 40-fold increase, respectively, on the inactivation rate of *C. albicans*.

4. Conclusions

This study presents an alternative approach for the disinfection of surface freshwater through the combined use of PMS/UV-A LED with or without M^{n+}. These stressors were tested on four microbial species, which varied in their ultra-structure and natural resistance mechanisms including the cell wall structure, endospore production and oxidative enzymes. The main conclusions that can be drawn from this study are:

- The photolytic activation of PMS through UV-A LED radiation achieves complete inactivation of the bacteria *E. coli*, *B. mycoides* and *S. aureus* using low dosages of PMS (0.1 mM) and at circumneutral pH. However, higher dosages of PMS (5 mM) are necessary to inactivate *C. albicans* due to its higher oxidative stress resistance.
- The inactivation rate of microorganisms can be increased during the first few minutes of contact time by the catalytic activation of PMS using a transition metal [Fe^{2+} or Co^{2+}]. However, the rapid catalytic consumption of sulphate radicals results in a lack of oxidant at later stages of the disinfection process and further dosing of PMS may be required.

- The combination of PMS with Co^{2+} obtained higher inactivation values for *S. aureus* and *C. albicans* than its combination with Fe^{2+}, which may be related to the fact that cobalt is more toxic than iron to eukaryotic cells.
- The gram-negative bacteria *E. coli* was more sensitive to the disinfection process than the gram-positive counterparts (*B. mycoides* and *S. aureus*) and the fungus *C. albicans*. Therefore, the use of *E. coli* as an indicator or model species for water disinfection studies, should be reconsidered because an efficient inactivation of *E. coli* does not necessarily imply an efficient inactivation of other pathogens.
- The oxidative stress generated through the complexity of PMS/M^{n+}/UV-A LED treatments triggered the formation of endospores in *B. mycoides*. Consequently, more demanding operational conditions may be required to reach the total inactivation of sporulated bacterial species.
- The Hom model satisfactorily fitted the inactivation results of all of the studied microorganisms. In addition, mathematical models based on Weibull distributions and Biphasic and Biphasic with Shoulder models accurately describe the inactivation curve of microorganisms in some of the studied treatments. These models are based on the hypothesis that the bacteria populations have sub-groups with different resilience to the treatments proposed.
- Finally, the use of UV-A LED radiation in treatment processes represent an attractive alternative to the use of conventional UV lamps, since LED are eco-friendly, present low operating cost and have a high-energy efficiency.

Acknowledgments

The authors are grateful to European Investment Funds by FEDER/COMPETE/POCI (POCI-01-0145-FEDER-006958) and National Funds by FCT under the projects UID/AGR/04033/2013 and UID/QUI/00616/2013. Project INNOFOOD - INNOvation in the FOOD sector through the valorization of food and agro-food by-products - NORTE-07-0124-FEDER-0000029, Project INTERACT – Integrative Research in Environment, Agro-Chains and Technology - NORTE-01-0145-FEDER-000017 and Project INNOVINE & WINE - Innovation Platform of Vine and Wine - NORTE-01-0145-FEDER-000038. Jorge Rodríguez-Chueca also acknowledges the funding provided by the Spanish Ministry of Economy and Competitiveness (MINECO) through the Juan de la Cierva-formación grant (No FJCI-2014-20195). Marco S. Lucas also acknowledges the funding provided by the European Union's Horizon 2020 research and innovation programme under the Marie Sklodowska-Curie grant agreement No 660969.

494 **References**

495 Acra A., Jurdi M., Mu'allem H., Karahagopian Y., Raffoul Z. 1990. Water Disinfection
496 by Solar Radiation: Assessment and Application, International Development
497 Research Centre (IDRC – Canada), PO Box 8500, Ottawa, Ont., Canada K1G 3H9.

498 Albert I., Mafart P. 2005. A modified Weibull model for bacterial inactivation. Int. J.
499 Food Microbiol. 100, 197-211.

500 Anipsitakis G.P., Dionysiou D.D. 2003. Degradation of organic contaminants in water
501 with sulfate radicals generated by the conjunction of peroxymonosulfate with cobalt.
502 Environ. Sci. Technol. 37, 4790–4797.

503 Anipsitakis G.P., Tufano T.P., Dionysiou D.D. 2008. Chemical and microbial
504 decontamination of pool water using activated potassium peroxymonosulfate. Water
505 Res. 42, 2899-2910.

506 Bailey M.M., Cooper W.J., Grant S.B. 2011. Grant. In situ disinfection of sewage
507 contaminated shallow groundwater: A feasibility study. Water Res. 45, 5641-5653.

508 Bandala E.R., Peláez M.A., Dionysiou D.D., Gelover S., Garcia J., Macías D. 2007.
509 Degradation of 2,4-dichlorophenoxyacetic acid (2,4-D) using
510 cobaltperoximonosulfate in Fenton-like process. Photochem. Photobiol. A 186, 357–
511 363.

512 Bigelow W.D., Esty J.R. 1920. The thermal death point in relation to typical
513 thermophilic organisms. J. Infect. Dis. 27, 602.

514 Blaha D., Arous S., Blériot C., Dorel C., Mandrand-Berthelot M., Rodrigue A. 2011.
515 The *Escherichia coli* metallo-regulator RcnR represses rcnA and rcnR transcription

516 through binding on a shared operator site: Insights into regulatory specificity towards
517 nickel and cobalt. Biochimie 93, 434-439.

518 Cabiscol E., Tamarit J., Ros J. 2000. Oxidative stress in bacteria and protein damage by
519 reactive oxygen species. Int. Microbiol. 3, 3–8.

520 Calderone R.A. 2002. Candida and Cadidiasis. ASM Press, USA.

521 Cerf O. 1977. A review: tailing of survival curves of bacterial spores. J. Appl. Bacteriol.
522 42, 1-19.

523 Conklin D.S., McMaster J.A., Culbertson M.R., Kung C. 1992. Kung. COT1, a gene
524 involved in cobalt accumulation in *Saccharomyces cerevisiae*. Mol. Cell. Biol. 12,
525 3678–3688.

526 Coroller L., Leguerinel I., Mettler E., Savy N., Mafart P. 2006. General model, based on
527 two mixed Weibull distributions of bacterial resistance, for describing various shapes
528 of inactivation curves. Appl. Environ. Microbiol. 72, 6493-6502.

529 Doederer K., Wolfgang G., Weinberg H.S., Farré M.J. 2014. Factors affecting the
530 formation of disinfection by-products during chlorination and chloramination of
531 secondary effluent for the production of high quality recycled water. Water Res. 48,
532 218–228.

533 Douglas L.J. 1988. *Candida* proteinases and candidiasis. Crit. Rev. Biotechnol. 8, 121–
534 129.

535 Eaton A.D., Clesceri L.S., Rice E.W., Greenberg A.E., Franson M.A.H. 2005. Standard
536 Methods for the Examination of Water and Wastewater. 21st ed. APA-AWWA-
537 WEF.

538 Ferro G., Fiorentino A., Alferez M.C., Polo-López M.I., Rizzo L., Fernández-Ibáñez P.
539 2015. Urban wastewater disinfection for agricultural reuse: effect of solar driven
540 AOPs in the inactivation of a multidrug resistant E. coli strain. Appl. Catal. B:
541 Environ. 178, 65-73.

542 Frohner I.E., Bourgeois C., Yatsyk K., Majer O., Kuchler K. 2009. *Candida albicans*
543 cell surface superoxide dismutases degrade host-derived reactive oxygen species to
544 escape innate immune surveillance. Mol. Microbiol. 71, 240–252.

545 Geeraerd A.H., Herremans C.H., Van Impe J.F. 2000. Structural model requirements to
546 describe microbial inactivation during a mild heat treatment. Int. J. Food Microbiol.
547 59, 185-209.

548 Geeraerd A.H., Valdramidis V.P., Van Impe J.F. 2005. GInaFiT, a freeware tool to
549 assess non-log-linear microbial survivor curves. Int. J. Food Microbiol. 102, 95-105.

550 Geeraerd A.H., Valdramidis V.P., Van Impe J.F. 2006. Erratum to “GInaFiT, a freeware
551 tool to assess non-log-linear microbial survivor curves”. Int. J. Food Microbiol. 110,
552 297.

553 Giannakis S., Papoutsakis S., Darakas E., Escalas-Cañellas A., Pétrier C., Pulgarin C.
554 2015. Ultrasound enhancement of near-neutral photo-Fenton for effective E. coli
555 inactivation in wastewater. Ultrason. Sonochem. 22, 515-526.

556 Grellier J., Rushton L., Briggs D., Nieuwenhuijsen M.J. 2015. Assessing the human
557 health impacts of exposure to disinfection by-products--a critical review of concepts
558 and methods. Environ. Int. 78, 61–81.

559 Hazen K.C., Cutler J.E. 1983. Isolation and purification of morphogenic autoregulatory
560 substance produced by *Candida albicans*. J. Biochem. 94, 777-783.

561 Hoerter J., Pierce A., Troupe C., Epperson J., Eisenstark A. 1996. Role of enterobactin
562 and intracellular iron in cell lethality during near-UV irradiation in *Escherichia coli*.
563 Photochem. Photobiol. 64, 537–541.

564 Hom L.W. 1972. Kinetics of chlorine disinfection in an ecosystem. J. Sanit. Eng. Div.
565 ASCE 98 (1), 183-193.

566 Imlay J.A. 2008. Cellular defenses against superoxide and hydrogen peroxide. Annu.
567 Rev. Biochem. 77 (1), 755–776.

568 ISO 5667-3:2012. Water quality: Sampling - Part 3: Preservation and handling of water
569 samples.

570 ISO 7027:1999. Water quality - Determination of turbidity.

571 ISO 7888:1985. Water quality - Determination of electrical conductivity.

572 Jiménez-López C., Lorenz M.C. 2013. Fungal Immune Evasion in a Model Host–
573 Pathogen Interaction: *Candida albicans* versus Macrophages. PLOS Pathog. 9, 1-4.

574 Kühn K.P., Chaberny I.F., Massholder K., Stickler M., Benz V.W., Sonntag H.G.,
575 Erdinger L. 2003. Disinfection of surfaces by photocatalytic oxidation with titanium
576 dioxide and UVA light. Chemosphere 53, 71-77.

577 LeChevallier M.W., Au K.K. 2004. Water treatment and pathogen control. Process
578 efficiency in achieving safe drinking water. World Health Organization, IWA
579 Publishing, London (United Kingdom).

580 Ma Z., Jacobsen F.E., Giedroc D.P. 2009. Coordination Chemistry of Bacterial Metal
581 Transport and Sensing. Chem. Rev. 109, 4644–4681.

582 Madigan M.T., Martinki J.M., Dunlap P.V., Clark D.P. 2012. Brock: Biology of
583 microorganisms. 13th Edition. Pearson Education. San Francisco (USA).

584 Mafart P., Couvert O., Gaillard S., Legurinel I. 2002. On calculating sterility in thermal
585 preservation methods: application of the Weibull frequency distribution model. Int. J.
586 Food Microbiol. 72, 107-113.

587 Ojkic N., López-Garrido J., Pogliano K., Endres R.G. 2016. Cell-wall remodeling
588 drives engulfment during *Bacillus subtilis* sporulation. Elife 5, e18657.

589 Parés R., Juárez A. 2002. Bioquímica de los microorganismos. Editorial Reverté S.A.,
590 Barcelona (Spain).

591 Pimentel C., Caetano S.M., Menezes R., Figueira I., Santos C.N., Ferreira R.B., Santos
592 M.A.S., Rodrigues-Pousada C. 2014. Yap1 mediates tolerance to cobalt toxicity in
593 the yeast *Saccharomyces cerevisiae*. Biochim. Biophys. Acta 1840, 1977–1986.

594 Reed R.H. 2004. The inactivation of microbes by sunlight: solar disinfection as a water
595 treatment process. Adv. Appl. Microbiol. 54, 333–365.

596 Richardson S.D., Plewa M.J., Wagner E.D., Schoeny R., Demarini D.M. 2007.
597 Occurrence, genotoxicity, and carcinogenicity of regulated and emerging disinfection
598 by-products in drinking water: a review and roadmap for research. Mutat. Res. 636,
599 178–242.

600 Rodrigue A., Effantin G., Mandrand-Berthelot M.A. 2005. Identification of rcnA
601 (yohM), a nickel and cobalt resistance gene in *Escherichia coli*. J. Bacteriol. 187,
602 2912-2916.

603 Rodríguez-Chueca J., Moreira S.I., Lucas M.S., Fernandes J.R., Tavares P.B., Sampaio
604 A., Peres J.A. 2017. Disinfection of simulated and real winery wastewater using
605 sulphate radicals: Peroxymonosulphate/transition metal/UV-A LED oxidation. J.
606 Clean. Prod. 149, 805–817.

607 Rook J.J. 1974. Formation of haloforms during chlorination of natural water. Water
608 Treat. Exam. 23 (2), 234–243.

609 Sattler U., Calsou P., Boiteux S., Salles B. 2000. Detection of oxidative base DNA
610 damage by a new biochemical assay. Arch. Biochem. Biophys. 376, 26–33.

611 Schaeffer A.B., Fulton M.A. 1933. A simplified method of staining endospores. Science
612 77, 194.

613 Serrano M., Real G., Santos J., Carneiro J., Moran C.P. Jr, Henriques A.O. 2011. A
614 negative feedback loop that limits the ectopic activation of a cell type–specific
615 sporulation sigma factor of *Bacillus subtilis*. PLOS Genetics 7, e1002220.

616 Spuhler D., Rengifo-Herrera J.A., Pulgarin C. 2010. The effect of Fe^{2+}, Fe^{3+}, H_2O_2 and
617 the photo-Fenton reagent at near neutral pH on the solar disinfection (SODIS) at low
618 temperatures of water containing *Escherichia coli* K12. Appl. Catal. B. 96, 126-141.

619 Stadler J.A., Schweyen R.J. 2002. The yeast iron regulon is induced upon cobalt stress
620 and crucial for cobalt tolerance. J. Biol. Chem. 277, 39649–39654.

621 Tyrrell R., Pourzand C., Brown J., Hejmadi V., Kvam E., Ryter S., Watkin R. 2000.
622 Cellular studies with UVA radiation: a role for iron. Radiat. Prot. Dosim. 91, 37–39.

623 Ullmann B.D., Myers H., Chiranand W., Lazzell A.L., Zhao Q. 2004. Inducible defense
624 mechanism against nitric oxide in *Candida albicans*. EC 3, 715–723.

United States Environmental Protection Agency. 1993. Method 410.4. The determination of chemical oxygen demand by semi-automated colorimetry.

Venieri D., Gounaki I., Binas V., Zachopoulos A., Kiriakidis G., Mantzavinos D. 2015. Inactivation of MS2 coliphage in sewage by solar photocatalysis using metal-doped TiO_2. Appl. Catal. B: Environ. 178, 54-64.

Wang X , Yi M, Liu H, Han Y, Yi H. 2017. Reactive oxygen species and Ca^{2+} are involved in cadmium-induced cell killing in yeast cells. Can. J. Microbiol. 63, 153-159.

Wang Y.R., Chu W. 2012. Photo-assisted degradation of 2,4,5-trichlorophenoxyacetic acid by Fe(II)-catalyzed activation of Oxone process: The role of UV irradiation, reaction mechanism and mineralization. Appl. Catal. B. 123-124, 151-161.

Wang Z.H., Yuan R.X., Guo Y.G., Xu L., Liu J.S. 2011. Effects of chloride ions on bleaching of azo dyes by Co^{2+}/oxone reagent: kinetic analysis. J. Hazard. Mater. 190, 1083–1087.

Wei G., Liang X., He Z., Liao Y., Xie Z., Liu P., Ji S., He H., Li D., Zhang J. 2015. Heterogeneous activation of Oxone by substituted magnetites $Fe_3{-}xMxO_4$ (Cr, Mn, Co, Ni) for degradation of Acid Orange II at neutral pH. J. Mol. Catal. A. Chem. 398, 86-94.

World Health Organization. 2008. Guidelines for drinking-water quality. Geneve (Switzerland).

Yu Z.Y., Kiwi-Minsker L., Renken A., Kiwi J. 2006. Detoxification of diluted azo-dyes at biocompatible pH with the Oxone/Co^{2+} reagent in dark and light processes. J. Mol. Catal. A. Chem. 252, 113–119.

FIGURE CAPTIONS

Figure 1. Inactivation of (a) *E. coli*; (b) *B. mycoides* and (c) *S. aureus* through the treatments PMS/UV-A LED.

Figure 2. Inactivation of (a) *E. coli*; (b) *B. mycoides* and (c) *S. aureus* after a single treatments PMS/M^{n+}/UV-A LED [M^{n+} = Fe^{2+} or Co^{2+}].

Figure 3. Inactivation of (a) *E. coli*; (b) *B. mycoides* and (c) *S. aureus* through the treatments PMS/M^{n+}/UV-A LED [M^{n+} = Fe^{2+} or Co^{2+}] with two reagent's additions.

Figure 4. Possible routes involved in photo-inactivation of *E. coli* (Gram-negative bacteria) through PMS/UV-A LED and PMS/M^{n+}/UV-A LED (Adapted from Ma et al. 2009 and Spuhler et al. 2010).

Figure 5. Structural differences between Gram-negative and Gram-positive bacteria.

Figure 6. Inactivation of *C. albicans* through the treatments (a) PMS/UV-A LED; (b) PMS/M^{n+}/UV-A LED [M^{n+} = Fe^{2+} or Co^{2+}].

662 **TABLE CAPTIONS**

663 **Table 1.** Mathematical kinetic models fitted to microbial populations after different
664 disinfection approaches. Log linear (L); Log linear with shoulder (LS); Log linear with
665 tail (LT); Log linear with shoulder and tail (LST); Hom (H); Weibull (W); Weibull with
666 tail (WT); Double Weibull (DT); Biphasic (B); Biphasic with shoulder (BS)

667 **Table 2.** Kinetic fitting parameters of *E. coli*, *B. mycoides* and *S. aureus* inactivation
668 after PMS/UV-A LED treatments.

669 **Table 3.** Kinetic fitting parameters of *E. coli*, *B. mycoides* and *S. aureus* inactivation
670 after PMS/M^{n+}/UV-A LED treatments.

671 **Table 4.** Kinetic fitting parameters of *E. coli*, *B. mycoides* and *S. aureus* inactivation
672 after PMS/M^{n+}/UV-A LED treatments with two different additions of reagents.

673 **Table 5.** Kinetic fitting parameters of *C. albicans* inactivation after PMS/UV-A LED
674 and PMS/M^{n+}/UV-A LED treatments.

675

Table 1

Kinetic model	Equation	Parameters	Reference
L	N	k	Bigelow and Esty, 1920
LS	$N - N_0 \cdot e^{-k \cdot t} \cdot \frac{e^{k \cdot Sl}}{}$	k, Sl	Geeraerd et al., 2000
LT	$N = (N_0 - N_{res}) \cdot e^{-k \cdot t}$	k, N_{res}	Geeraerd et al., 2000
LST	$N = (N_0 - N_{res}) \cdot \frac{e^{-k \cdot t} \cdot e^{k \cdot Sl}}{(1 + e^{k \cdot Sl - 1}) \cdot e^{-k \cdot t}}$	k, N_{res}, Sl	Geeraerd et al., 2000
H	$Log \frac{N_t}{N_0} = -k \cdot C^n \cdot t^m$	k, n, m	Hom, 1972
W	$Log \frac{N_t}{N_0}$	δ, p	Mafart et al., 2002
WT	$N = (N_0 - N_{res}) \cdot 10^{-(\frac{t}{\delta})^p}$	δ, p, N_{res}	Albert and Mafart, 2005
DT	$N(t) = \frac{N_0}{1 + 10^{\alpha}} \left[10^{-(\frac{t}{\delta_1})^{p_1 + \alpha}} \right.$	δ_1, δ_2, p_1, p_2, α	Coroller et al., 2006
B	$Log \frac{N_t}{N_0} = Log[P \cdot e^{-k_1 \cdot t} + (1 - P)$	P, k_1, k_2	Cerf, 1977
BS	$Log \frac{N_t}{N_0} = Log[f \cdot e^{-k_1 \cdot t} \cdot \frac{e^{k_1 \cdot S_1}}{1 + (e^{k_1 \cdot S_1} - 1) \cdot e^{-k_1 \cdot t}} + (1 - f) \cdot e^{-k_2 \cdot t}$	P, k_1, k_2, Sl	Geeraerd et al., 2005, 2006

Table 2

Kinetic model	*E. coli*			*B. mycoides*			*S. aureus*		
	k_1 (min^{-1})/ δ_1 (min)	k_2 (min^{-1})/ δ_2 (min)	R^2/RMSD	k_1 (min^{-1})/ δ_1 (min)	k_2 (min^{-1})/ δ_2 (min)	R^2/RMSD	k_1 (min^{-1})/ δ_1 (min)	k_2 (min^{-1})/ δ_2 (min)	R^2/RMSD
0.1 mM PMS/UV-A LED									
L (k)	0.18	-	0.97 / 0.51	0.12	-	0.97/0.30	0.10	-	0.88/0.69
H (k)	0.39	-	0.99 / 0.09	0.06		0.97/0.26	0.33	-	0.96/0.37
LT (k)	-	-	-	-	-	-	0.16	-	0.98/0.31
W (δ)	10.00	-	0.98 / 0.44	19.73	-	0.97/0.34	5.28	-	0.96/0.44
WT (δ)	-	-	-	-	-	-	12.45	-	0.98/0.33
DW (δ)	4.35	6.02	0.99 / 0.13	17.41	65.87	0.99/0.12	-	-	-
B (k)	0.34	0.14	0.99 / 0.20	-	-	-	0.16	0.02	0.98/0.32
BS (k)	0.39	0.14	0.99 / 0.28	-	-	-	0.17	0.02	0.98/0.38
0.1 mM PMS/Dark									
L (k)	0.13	-	0.98 / 0.32	0.05	-	0.94 / 0.14	0.06	-	0.89/0.39
H (k)	0.18	-	0.98 / 0.18	0.15	-	0.98 / 0.07	0.003	-	0.95/0.29
LS (k)	-	-	-	-	-	-	0.09	-	0.96/0.27
W (δ)	12.10	-	0.98 / 0.31	34.81	-	0.98 / 0.09	66.92	-	0.97/0.24
DW (δ)	0.39	21.03	0.99 / 0.27				-	-	-
B (k)	-	-	-	0.08	0.00	0.98/0.11	-	-	-
BS (k)	-	-	-	0.08	0.00	0.98/0.14	-	-	-

Table 3

Kinetic model	*E. coli*			*B. mycoides*			*S. aureus*		
	k_1 (min^{-1})/ δ_1 (min)	k_2 (min^{-1})/ δ_2 (min)	R^2/RMSD	k_1 (min^{-1})/ δ_1 (min)	k_2 (min^{-1})/ δ_2 (min)	R^2/RMSD	k_1 (min^{-1})/ δ_1 (min)	k_2 (min^{-1})/ δ_2 (min)	R^2/RMSD
0.1 mM PMS/0.1 mM Fe(II)/UV-A LED									
L (k)	-	-	-	-	-	-	0.06	-	0.97 / 0.21
H (k)	2.12	-	0.93 / 0.65	1.06	-	0.98 / 0.07	0.05	-	0.97 / 0.19
LST (k)	-	-	-	-	-	-	0.09	-	0.98 / 0.19
W (δ)	0.07	-	0.93 / 0.82	-	-	-	35.50	-	0.97 / 0.23
WT (δ)	-	-	-	-	-	-	40.34	-	0.98 / 0.20
DW (δ)	-	-	-	-	-	-	42.93	116.86	0.99 / 0.17
B (k)	0.39	0.002	0.92 / 0.95	0.21	0.01	0.90 / 0.45	-	-	-
BS (k)	-	-	-	-	-	-	0.14	0.03	0.99 / 0.19
0.1 mM PMS/0.1 mM Co(II)/UV-A LED									
H (k)	2.39	-	0.97 / 0.38	0.80	-	0.93 / 0.25	1.54	-	0.97 / 0.30
LT (k)	-	-	-	-	-	-	0.15	-	0.88 / 0.76
W (δ)				3.33	-	0.93 / 0.31	0.32	-	0.97 / 0.36
B (k)	7.21	0.09	0.95 / 0.67	0.16	0.02	0.90 / 0.42	5.16	0.07	0.97 / 0.38

Table 4

Kinetic model	*E. coli*			*B. mycoides*			*S. aureus*		
	k_1 (min^{-1})/ δ_1 (min)	k_2 (min^{-1})/ δ_2 (min)	R^2/RMSD	k_1 (min^{-1})/ δ_1 (min)	k_2 (min^{-1})/ δ_2 (min)	R^2/RMSD	k_1 (min^{-1})/ δ_1 (min)	k_2 (min^{-1})/ δ_2 (min)	R^2/RMSD
0.1 mM PMS/0.1 mM Fe(II)/UV-A LED [2 additions]									
L (k)	-	-	-	-	-	-	0.13	-	0.97 / 0.48
H (k)	1.92	-	0.95 / 0.49	0.68	-	0.98 / 0.04	0.11	-	0.98 / 0.37
LT (k)	0.31	-	0.91 / 0.83	-	-	-	0.15	-	0.98 / 0.37
LST (k)	-	-	-	-	-	-	0.16	-	0.98 / 0.40
W (δ)	-	-	-	-	-	-	15.17	-	0.97 / 0.49
WT (δ)	-	-	-	-	-	-	21.18	-	0.98 / 0.40
DW (δ)	-	-	-	-	-	-	21.94	66.89	0.99 / 0.28
B (k)	0.31	0.01	0.91 / 0.92	-	-	-	0.16	0.06	0.99 / 0.36
BS (k)	-	-	-	-	-	-	0.17	0.06	0.99 / 0.39
0.1 mM PMS/0.1 mM Co(II)/UV-A LED [2 additions]									
H (k)	2.38	-	0.97 / 0.30	$1.37 \cdot 10^{-5}$	-	0.95 / 0.13	2.12	-	0.98 / 0.26
LS (k)	-	-	-	0.09	-	0.98 / 0.09	-	-	-
W (δ)	0.01	-	0.97 / 0.38	3.80	-	0.98 / 0.10	-	-	-
WT (δ)	1.24	-	0.90 / 0.79	-	-	-	-	-	-
DW (δ)	-	-	-	0.98	105.88	0.97 / 0.12	-	-	-
B (k)	6.11	0.07	0.93 / 0.67	-	-	-	1.04	0.05	0.91 / 0.77
BS (k)	-	-	-	-	-	-	-	-	-

Table 5

Kinetic model	*C. albicans*		
	k_1 (min^{-1})/ δ_1 (min)	k_2 (min^{-1})/ δ_2 (min)	R^2/RMSD
5 mM PMS/UV-A LED			
L (*k*)	0.11	-	0.96 / 0.47
H (*k*)	0.09	-	0.95 / 0.44
LS (*k*)	0.11	-	0.96 / 0.50
W (δ)	20.19	-	0.96 / 0.51
WT (δ)	32.87	-	0.98 / 0.34
B (*k*)	0.12	$3.48 \cdot 10^{-3}$	0.97 / 0.48
5 mM PMS/2.5 mM Fe (II)/UV-A LED			
H (*k*)	0.90	-	0.94 / 0.47
B (*k*)	0.21	0.00	0.98 / 0.14
BS (*k*)	0.21	0.00	0.98 / 0.18
5 mM PMS/2.5 mM Co (II)/UV-A LED			
H (*k*)	4.23	-	0.99 / 0.15
LT (*k*)	10.07	-	0.96 / 0.38
5 mM PMS/2.5 mM Fe (II)/UV-A LED (2 additions)			
H (*k*)	1.46	-	0.88 / 0.77
B (*k*)	0.37	0.00	0.97 / 0.54

Figure 1

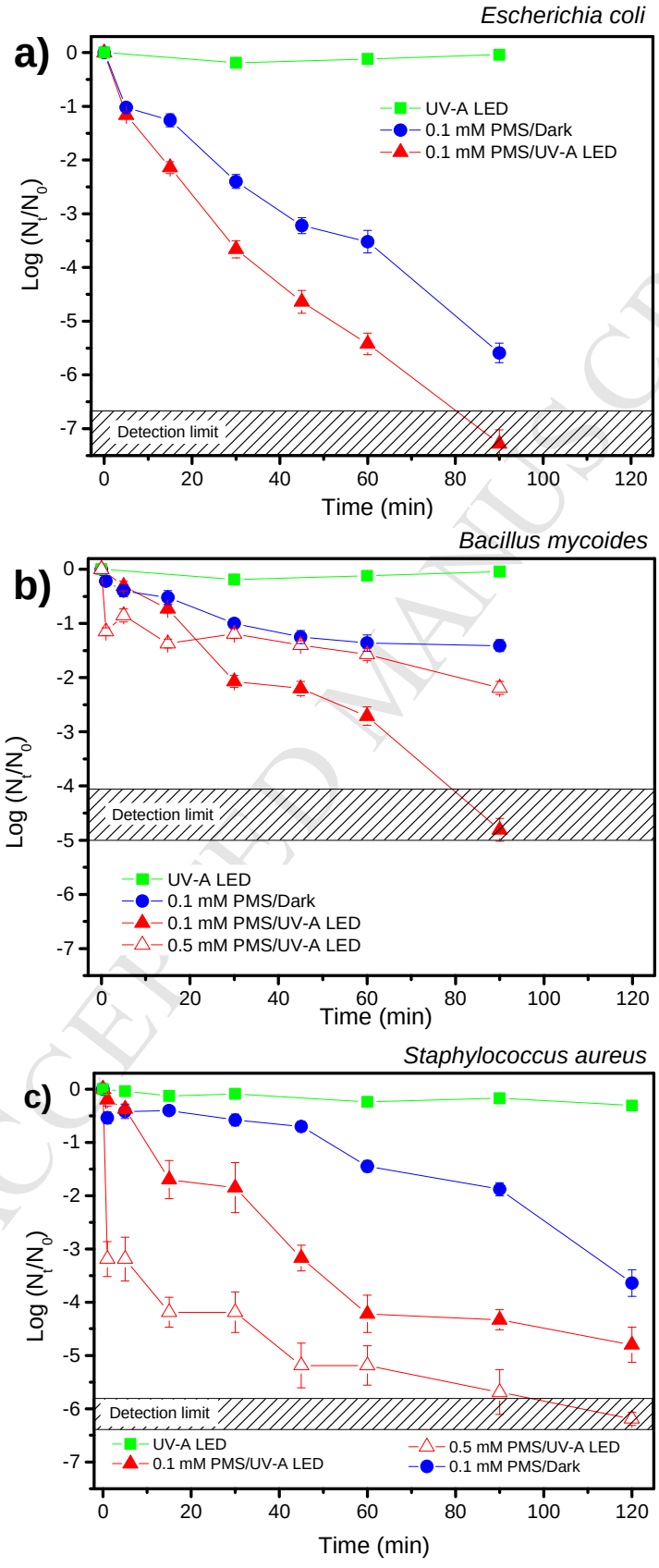

Figure 2

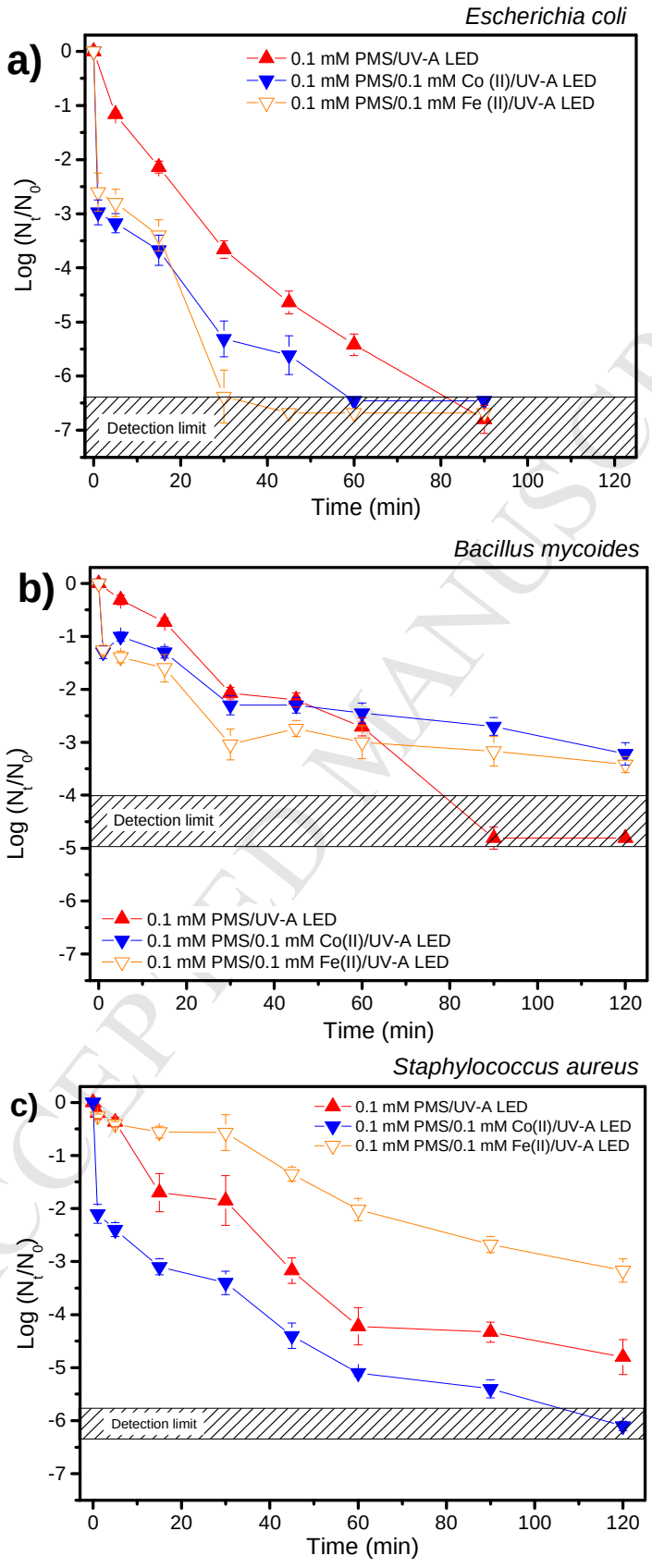

Figure 3

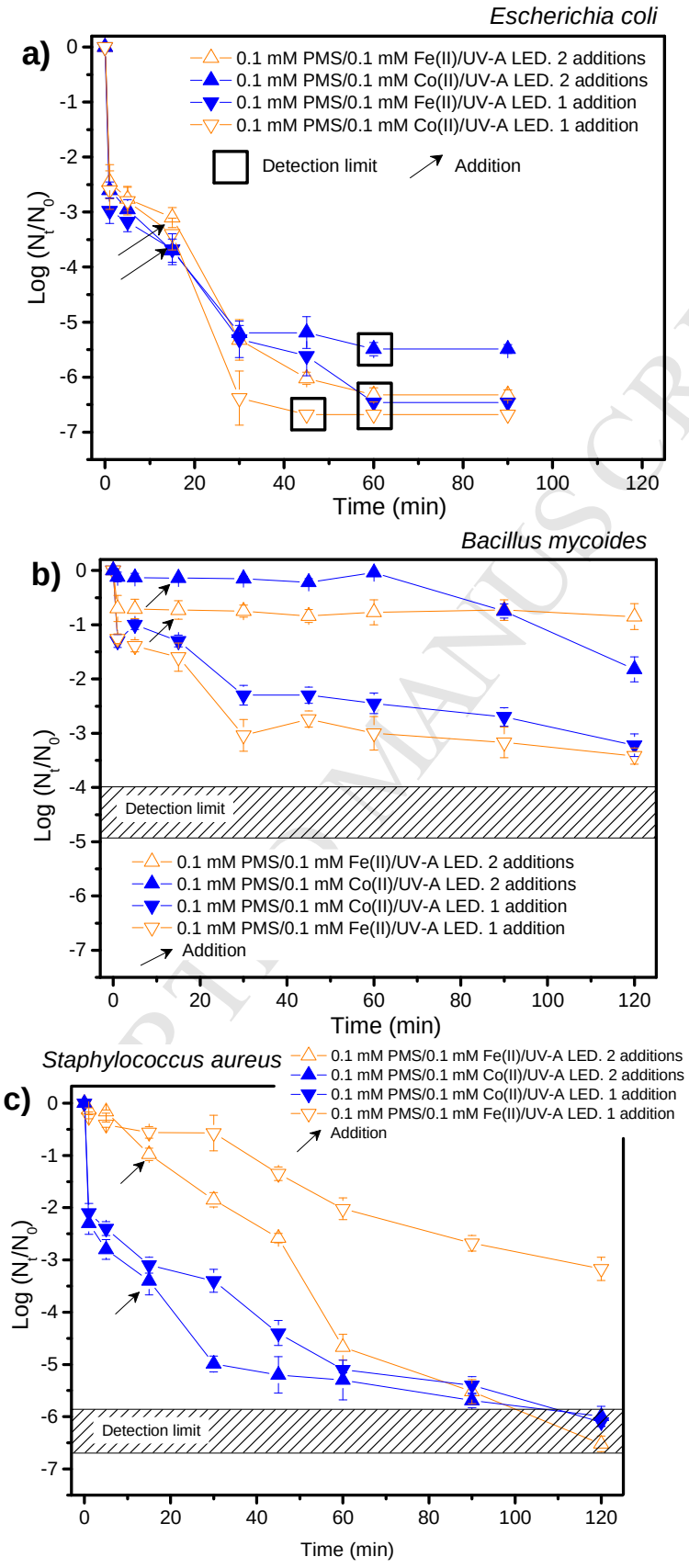
Escherichia coli
a)
0.1 mM PMS/0.1 mM Fe(II)/UV-A LED. 2 additions
0.1 mM PMS/0.1 mM Co(II)/UV-A LED. 2 additions
0.1 mM PMS/0.1 mM Fe(II)/UV-A LED. 1 addition
0.1 mM PMS/0.1 mM Co(II)/UV-A LED. 1 addition
Detection limit
Addition
Log (N_t/N_0)
Time (min)
Bacillus mycoides
b)
Detection limit
0.1 mM PMS/0.1 mM Fe(II)/UV-A LED. 2 additions
0.1 mM PMS/0.1 mM Co(II)/UV-A LED. 2 additions
0.1 mM PMS/0.1 mM Co(II)/UV-A LED. 1 addition
0.1 mM PMS/0.1 mM Fe(II)/UV-A LED. 1 addition
Addition
Log (N_t/N_0)
Time (min)
Staphylococcus aureus
c)
0.1 mM PMS/0.1 mM Fe(II)/UV-A LED. 2 additions
0.1 mM PMS/0.1 mM Co(II)/UV-A LED. 2 additions
0.1 mM PMS/0.1 mM Co(II)/UV-A LED. 1 addition
0.1 mM PMS/0.1 mM Fe(II)/UV-A LED. 1 addition
Addition
Detection limit
Log (N_t/N_0)
Time (min)

Figure 4

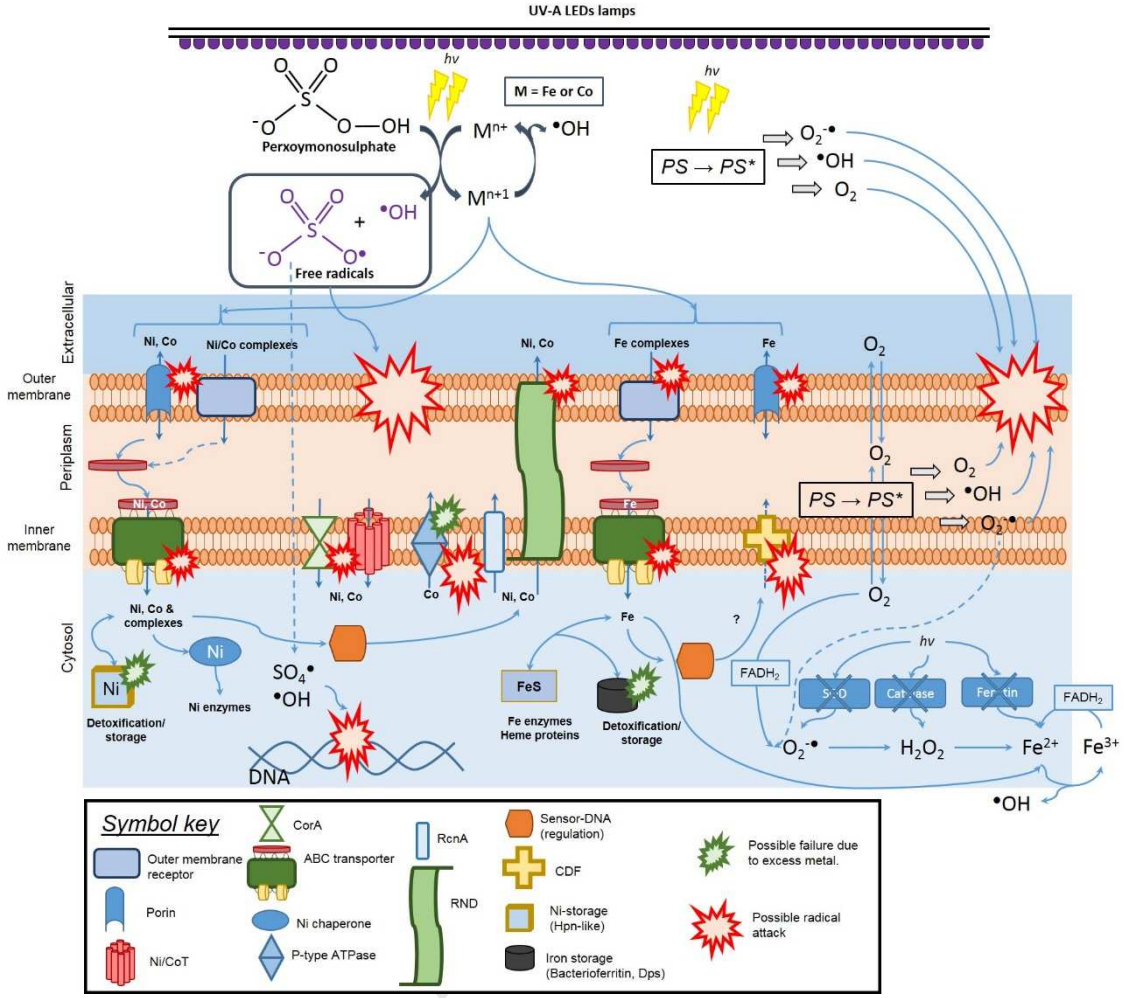
UV-A LEDs lamps
hv
M = Fe or Co
Peroxymonosulphate
Free radicals
PS → PS*
Extracellular
Outer membrane
Periplasm
Inner membrane
Cytosol
Ni, Co
Ni/Co complexes
Fe complexes
Fe
Ni, Co & complexes
Detoxification/ storage
Ni enzymes
DNA
FeS
Fe enzymes Heme proteins
FADH2
Catalase
Ferritin
Symbol key
Outer membrane receptor
Porin
Ni/CoT
CorA
ABC transporter
Ni chaperone
P-type ATPase
RcnA
RND
Sensor-DNA (regulation)
CDF
Ni-storage (Hpn-like)
Iron storage (Bacterioferritin, Dps)
Possible failure due to excess metal.
Possible radical attack

Figure 5

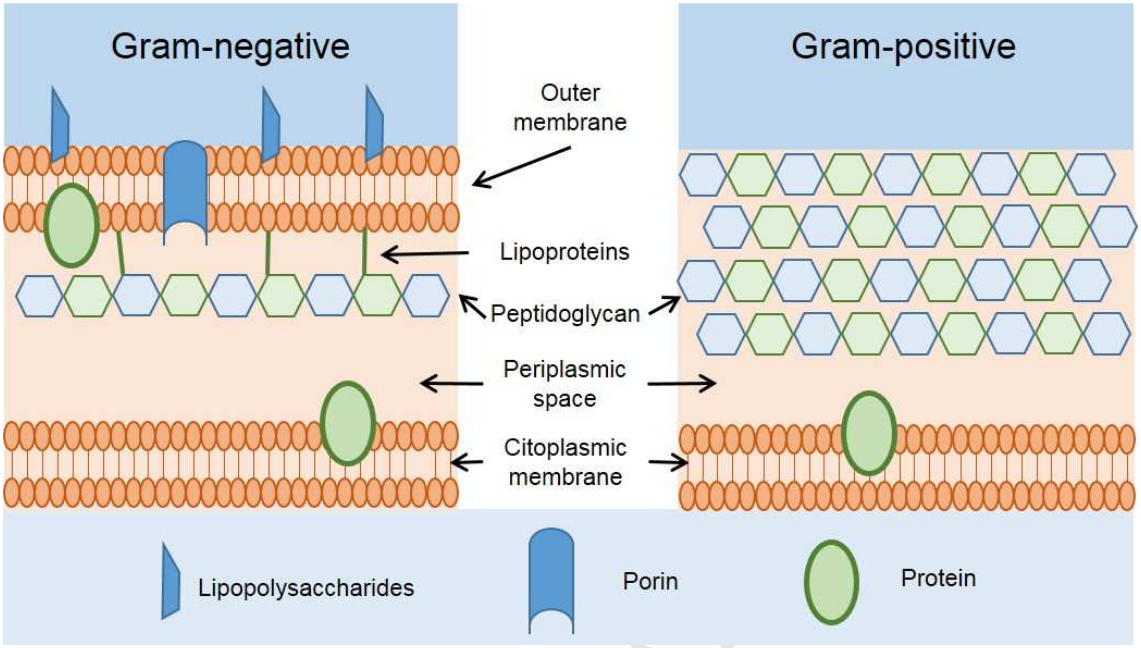

Figure 6

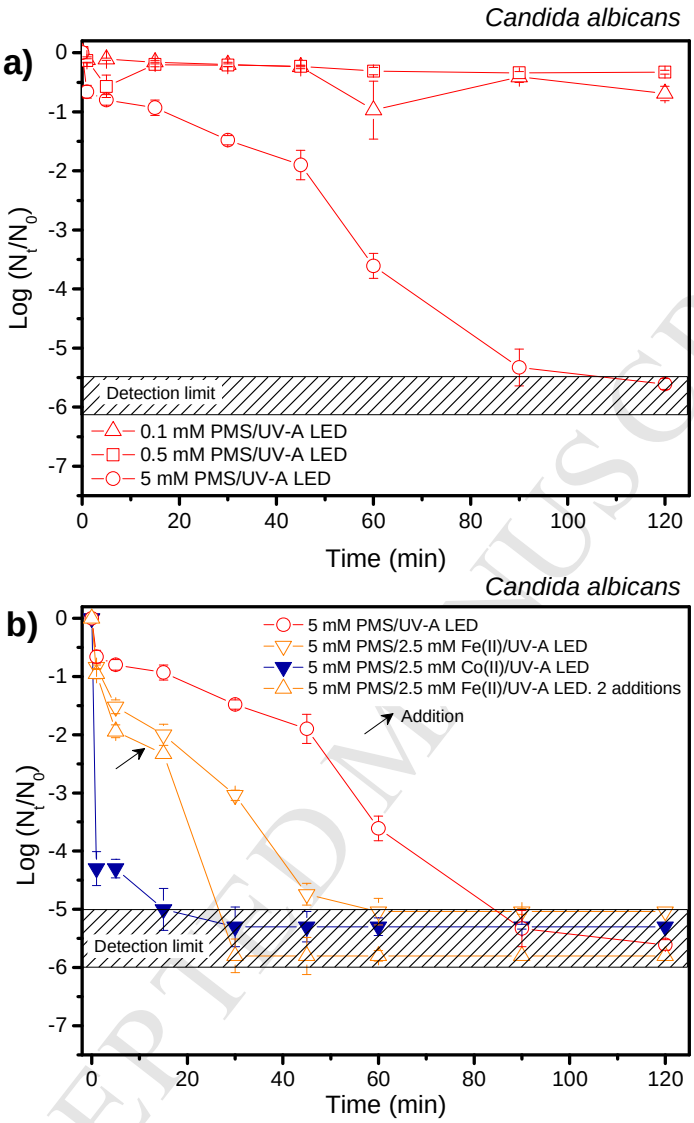

Highlights

- Inactivation of pathogens with sulphate radicals and UV-A LEDs
- *E. coli*, *B. mycoides* and *S. aureus* inactivated with low dosages of PMS and at circumneutral pH
- Hom model fitted the inactivation results of all studied microorganisms
- Sulphate radical mechanism of attack over *E. coli*